

Geophysical Research Letters

RESEARCH LETTER

10.1029/2018GL081339

Key Points:

- Low-temperature hydrated salts from the Canadian Arctic provide geochemical and spectral analogues for european surface material
- Qualitatively different deposits can form from fluids with similar major ion chemistry
- Endogenic sulfates on Europa would not rule out a chloride-dominated ocean

Supporting Information:

- Supporting Information S1
- Table S1
- Table S2
- Table S3
- Table S4

Correspondence to:

M. G. Fox-Powell,
mgfp@st-andrews.ac.uk

Citation:

Fox-Powell, M. G., Osinski, G. R., Applin, D., Stromberg, J. M., Gázquez, F., Cloutis, E., et al. (2019). Natural analogue constraints on Europa's non-ice surface material. *Geophysical Research Letters*, 46. <https://doi.org/10.1029/2018GL081339>

Received 17 NOV 2018

Accepted 18 APR 2019

Accepted article online 29 APR 2019

Natural Analogue Constraints on Europa's Non-ice Surface Material

Mark G. Fox-Powell¹ , Gordon R. Osinski² , Daniel Applin³, Jessica M. Stromberg^{3,4} , Fernando Gázquez^{1,5}, Ed Cloutis³ , Elyse Allender¹ , and Claire R. Cousins¹ 

¹Centre for Exoplanet Science, School of Earth and Environmental Sciences, University of St Andrews, St Andrews, UK,

²Centre for Planetary Science and Exploration, Department of Earth Sciences, University of Western Ontario, London,

Ontario, Canada, ³Department of Geography, University of Winnipeg, Winnipeg, Manitoba, Canada, ⁴Now at CSIRO

Mineral Resources, Perth, Western Australia, Australia, ⁵Now at Department of Geology and Biology, University of

Almería, Almería, Spain

Abstract Non-icy material on the surface of Jupiter's moon Europa is hypothesized to have originated from its subsurface ocean and thus provide a record of ocean composition and habitability. The nature of this material is debated, but observations suggest that it comprises hydrated sulfate and chloride salts. Analogue spectroscopic studies have previously focused on single-phase salts under controlled laboratory conditions. We investigated natural salts from perennially cold (<0 °C) hypersaline springs and characterized their reflectance properties at 100, 253, and 293 K. Despite similar major ion chemistry, these springs form mineralogically diverse deposits, which when measured at 100 K closely match reflectance spectra from Europa. In the most sulfate-rich samples, we find that spectral features predicted from laboratory salts are obscured. Our data are consistent with sulfate-dominated european non-icy material and further show that the emplacement of endogenic sulfates on Europa's surface would not preclude a chloride-dominated ocean.

Plain Language Summary Europa, a moon of Jupiter, has become a priority target in the search for life off the Earth, due to the presence of a liquid water ocean under its icy shell. Salts on the moon's surface might originate from this ocean and therefore offer a way of studying the ocean without requiring direct access. Our knowledge of these salts comes from comparing spacecraft measurements to pure salts produced in laboratories. We have studied natural salts from hypersaline springs in the Canadian Arctic as an alternative, complementary approach. Measuring samples from these deposits at european surface temperatures, several unexpected properties were observed, including the absence of spectral details predicted by previous laboratory studies. This challenges some of the estimates of european surface composition. Natural analogues such as these will form part of an integrative approach to understanding data from upcoming missions, such as the National Aeronautics and Space Administration's (NASA) Europa Clipper and the European Space Agency's JUPITER ICy moons Explorer.

1. Introduction

In the coming decade, the European Space Agency's JUPITER ICy moons Explorer (JUICE) and the National Aeronautics and Space Administration (NASA) Europa Clipper will study the icy moon Europa to better understand its surface and subsurface activity and potential habitability. Europa hosts a liquid water layer beneath an icy crust (Carr et al., 1998), with a depth of up to 100 km (Nimmo & Pappalardo, 2016). The interaction between this ocean and a silicate core could generate the necessary chemical conditions for life, meaning Europa may harbor the largest habitable volume of water in the solar system (Nimmo & Pappalardo, 2016).

Constraining ocean composition is crucial to understanding the evolution and astrobiological potential of Europa. The european surface is predominantly water ice (Carlson et al., 2009); however, spatially heterogeneous, non-icy material exists, first studied by the Galileo spacecraft's Near-Infrared Mapping Spectrometer (NIMS; McCord et al., 1999). This material is hypothesized to have originated, either wholly or partly, from the subsurface ocean, becoming frozen into exhumed ice or delivered directly to the surface through cryovolcanism (Howell & Pappalardo, 2018; Prockter et al., 2017; Schmidt et al., 2011). The existence of putative cryovolcanic plumes on Europa (Jia et al., 2018; Roth et al., 2014) further suggests that material from Europa's interior is actively emplaced onto the surface. This surface material can provide a record of ocean chemistry accessible to orbital or landed spacecraft.

Multiple observations of Europa's non-icy material exist, showing visible near-infrared (vis-NIR) evidence for hydrated compounds (Brown & Hand, 2013; Carlson et al., 2005; Dalton et al., 2012; Fischer et al., 2015, 2016; Ligier et al., 2016; McCord et al., 1999). Such material can form through exogenic and radiolytic processes, salt precipitation from subsurface brines, or a combination of these two mechanisms. Previous studies have attempted to explain the shape of europian non-icy spectra with numerical linear mixes of pure salt spectra (Carlson et al., 2005; Dalton, 2007; Ligier et al., 2016) or with experimentally produced salt assemblages (Orlando et al., 2005). Based on these works, hydrated sulfates such as mirabilite ($\text{Na}_2\text{SO}_4 \cdot 10\text{H}_2\text{O}$) and sulfuric acid hydrate have been proposed as major components of deposits on the trailing hemisphere (Carlson et al., 2005; Dalton et al., 2012; Shirley et al., 2010), whereas chloride salts may contribute to spectral signatures of "chaos" regions (Brown & Hand, 2013; Fischer et al., 2016).

The study of natural analogues provides a complementary approach, particularly for understanding spectral behavior of mineralogically heterogeneous precipitates. Axel Heiberg Island (AHI) in the Canadian Arctic hosts unique hypersaline, subzero ($<0^\circ\text{C}$) springs that precipitate hydrated sodium sulfates and chloride salts, along with other low-temperature phases (Battler et al., 2013; Ward & Pollard, 2018). We investigated the vis-NIR spectral properties and geochemical context of these natural hydrated salt assemblages and discuss their relevance for the exploration of Europa.

2. Field Areas

AHI, Nunavut, Canada, (Figure 1a) hosts Carboniferous evaporite diapirs (Harrison & Jackson, 2014) and thick (>400 m) permafrost (Andersen et al., 2002). Associated with the diapirs are anoxic, perennially low-temperature (-5 to 8°C) hypersaline (>10 wt. %) springs that form assemblages of hydrated sulfate and chloride salts (Battler et al., 2013; Pollard et al., 1999). The precipitation of these Europa-relevant phases makes these springs compelling natural laboratories for understanding analogous deposits on Europa. The waters of three springs, Lost Hammer (LH), Color Peak (CP), and Stolz (STZ), were sampled along with their associated salt deposits in July 2017 (Figure 1; for further details of geologic setting see Battler et al., 2013, and Ward & Pollard, 2018).

2.1. LH

LH Spring (also known as Wolf Spring; Battler et al., 2013; 79.076856, -90.210472) emerges as a single outlet from the valley floor, approximately 500 m from the base of Wolf Diapir (Figure 1b). A large dome of salt exists around the vent, flanked by a salt apron with terracing and layering. Brine samples and measurements were taken from the outlet and at two downstream points. Salt samples were taken from within the outlet dome and from the salt apron (Figure S1 in the supporting information).

2.2. CP

CP springs (79.38, -91.27) emerge as several outlets from the side of CP Diapir (Figure 1c). Precipitates exist as sintered terraces exhibiting green and black coloration. White crusts are visible at the edges of channels and pools. Brine samples and measurements were taken at five spring outlets, and mineral samples were taken from terraces and peripheral precipitates (Figure S1).

2.3. STZ

STZ springs (79.090117, -87.048248) emerge from two outlets on STZ Diapir (Figure 1). The springs meet at a confluence 20-m downstream from the outlets, precipitating an extensive salt apron with an approximate thickness of 5 m and downslope extent of ~ 800 m. During summer, the drainage streams flow under this apron into a "salt cave." Salts form gray and white terraces (Figure 1e), with the dry remains of large (~ 10 -m diameter) pools on the apron. Brine samples and measurements were taken at both outlets and at the confluence. Salts were sampled at the entrance to the salt cave and from the apron surface (Figure S1).

3. Materials and Methods

3.1. Sampling

Brine samples were 0.22 μm filtered into four 15-ml aliquots for stable isotopes, anion and cation analysis, and aqueous sulfide measurements. Samples for cation analyses were acidified to a final concentration of 1% HNO_3 . Temperature, pH, and dissolved oxygen concentrations were measured using a Mettler Toledo

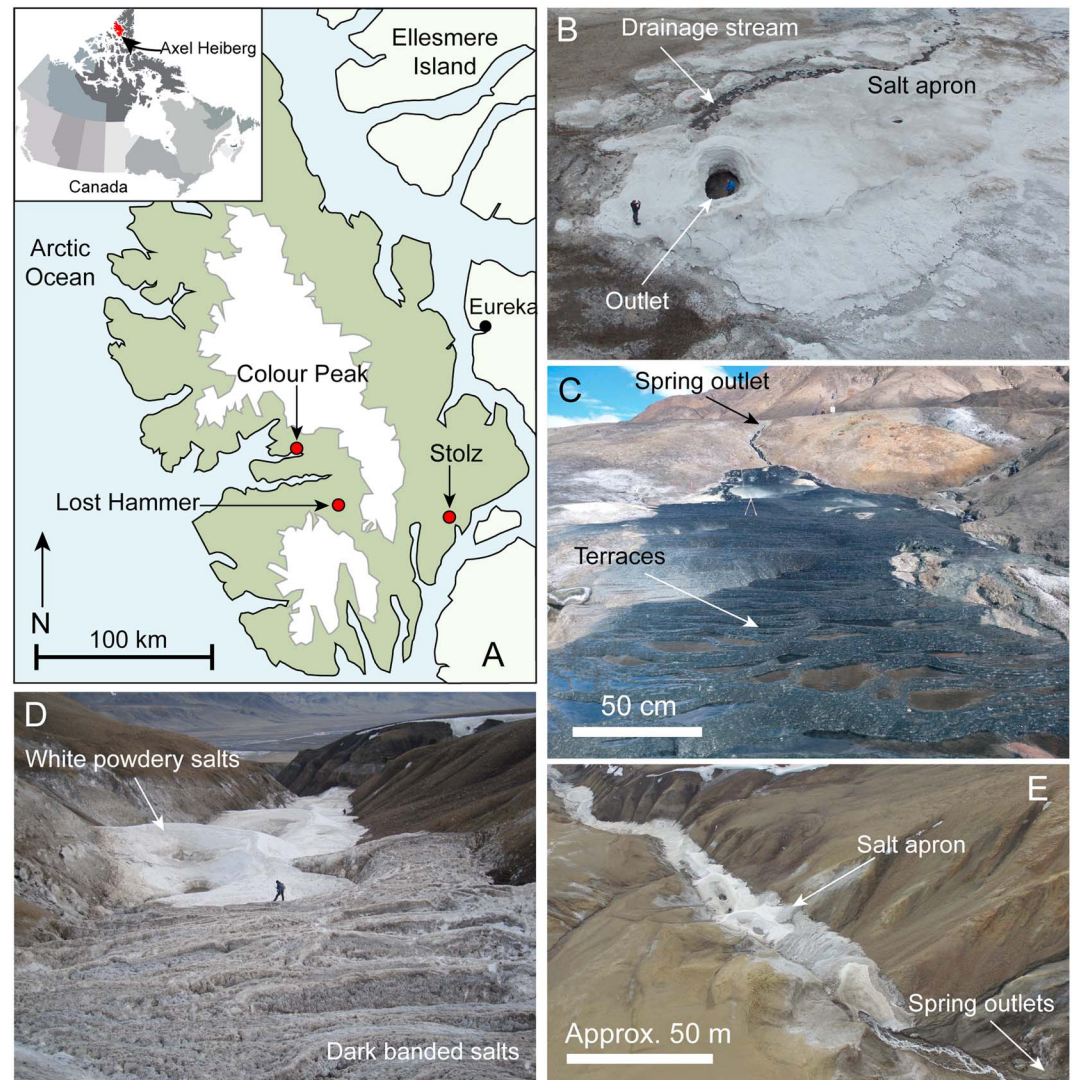


Figure 1. (a) Map of Axel Heiberg Island, location of the three springs studied, and ice caps (white). (b) Aerial view of Lost Hammer spring, showing outlet and salt apron. Person for scale. (c) Terraces at Color Peak springs and outlet channel. (d) Salt apron at Stolz Spring. Person for scale. (e) Aerial view of Stolz Springs, showing the outlets on the side of Stolz Diapir

FiveGo probe. Salt mineral precipitates were collected into sample bags and stored at ambient arctic temperatures, shipped chilled (4 °C), and stored at 4 °C until analysis.

3.2. Quantification of Major Ions

Cations in spring fluids were measured with ICP-AES using a Prodigy7 (Teledyne-Leeman) AES system at the Open University, UK. Chloride and sulfate were measured in triplicate with ion chromatography using a Metrohm 930 IC system fitted with a 150-mm Metrosep Asupp5 separation column (4-mm bore). Relative standard deviations of triplicate measurements were $\leq 0.1\%$ for all measured anions. Brines were diluted by a factor between 10^3 and 10^4 in ultrapure deionized water prior to analysis. Aqueous sulfide was quantified spectrophotometrically in triplicate using the methylene blue assay (Cline, 1969).

3.3. Oxygen and Hydrogen Isotopes in Waters

Water bound ^{16}O , ^{18}O , H, and D were measured simultaneously by cavity ring-down spectrometry using a L2140-i Picarro water isotope analyzer at the University of St. Andrews, UK. Seven repeat measurements

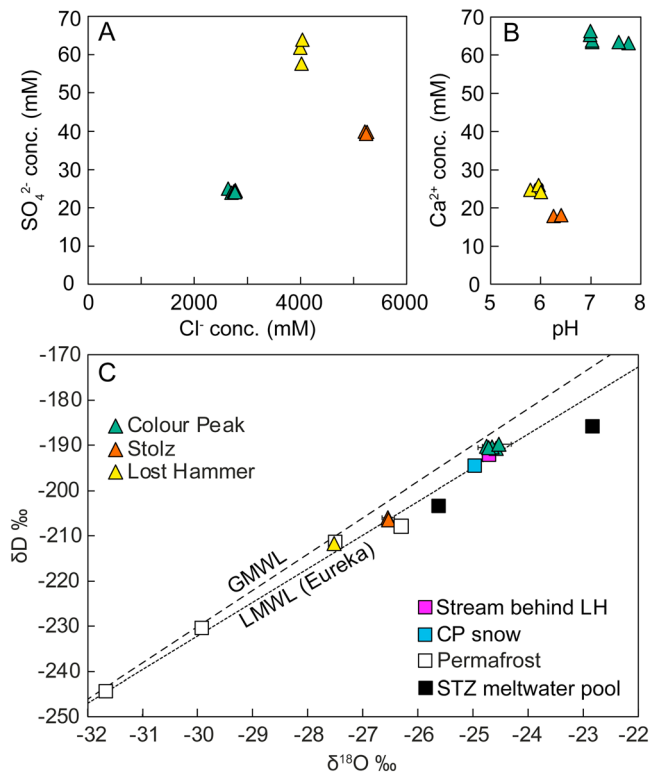


Figure 2. Axel Heiberg Island spring geochemistry. (a) Major anions. (b) Calcium concentration versus pH. (c) Water isotopic composition of the springs and potential source waters. Global (G) and local (L) meteoric water lines (MWL) plotted for reference (Pollard et al., 1999). LH = Lost Hammer; CP = Color Peak; STZ = Stolz.

were averaged for each sample, with a typical precision of $\pm 0.03\text{‰}$ for $\delta^{18}\text{O}$ and 0.3‰ for δD (1 SD.). See supporting information methods for more details.

3.4. XRD

Powder X-ray diffraction (XRD) patterns were recorded at Drochaid Research Services, Ltd. (St Andrews, UK) at room temperature from 10° to 110° (2θ) using a Panalytical X'Pert Pro X-ray diffractometer. Samples were equilibrated to room temperature and crushed as finely as possible prior to analysis. In an effort to retain hydrated phases, samples were not fully dried; therefore, sieving and grain size normalization was not possible. Because of this, Rietveld refinements are taken as semiquantitative, indicative of major and minor phases. See supporting information methods for more details.

3.5. Vis-NIR Reflectance Spectroscopy

Vis-NIR (0.35 to $2.5\ \mu\text{m}$) spectra from salt precipitates were collected at three temperatures: 293 K (room temperature), 253 K, and approximately 100 K (simulating european surface temperature; Nimmo & Pappalardo, 2016). Spectra were acquired with an Analytical Spectral Devices FieldSpec Pro HR spectrometer at the Planetary Spectroscopy Facility, University of Winnipeg. See supporting information methods for more details. Samples at 253 K were frozen in a chest freezer, followed by active cooling with a Pelletier cooler after Bramble et al. (2014). Samples measured at 100 K were held in an aluminum sample cup that was immersed in liquid nitrogen and equilibrated until the liquid nitrogen ceased to boil vigorously.

The 100-K spectra were resampled to (1) Galileo NIMS spectral resolution, to precisely match bandpasses in the G1ENNHILAT01 observation presented by Dalton et al. (2005) and others, (2) the Europa Clipper Mapping Infrared Spectrometer for Europa (MISE) spectral resolution (10-nm sampling from 0.8 to $5\ \mu\text{m}$; Blaney et al., 2015), and (3) the JUICE Moons and Jupiter Imaging Spectrometer (MAJIS) spectral resolution (2.3-nm sampling from 0.4 to $1.7\ \mu\text{m}$ and 6.6-nm sampling from 1.7 to $5.7\ \mu\text{m}$; Langevin et al., 2013).

Mapping Infrared Spectrometer for Europa (MISE) spectral resolution (10-nm sampling from 0.8 to $5\ \mu\text{m}$; Blaney et al., 2015), and (3) the JUICE Moons and Jupiter Imaging Spectrometer (MAJIS) spectral resolution (2.3-nm sampling from 0.4 to $1.7\ \mu\text{m}$ and 6.6-nm sampling from 1.7 to $5.7\ \mu\text{m}$; Langevin et al., 2013).

3.6. Spectral Mixing

To investigate the loss of spectral detail caused by the presence of anhydrous phases, linear spectral mixes were generated to compare directly with the LH outlet sample, which has four phases in XRD patterns: anhydrous thenardite (Na_2SO_4) and halite (NaCl) and their hydrous counterparts mirabilite ($\text{Na}_2\text{SO}_4 \cdot 10\text{H}_2\text{O}$) and hydrohalite ($\text{NaCl} \cdot 2\text{H}_2\text{O}$). Semiquantitative XRD indicates sulfates form the major salt phase (approximately 80%) with a minor chloride salt phase (approximately 20%), and this ratio was maintained in each mix, varying the anhydrous component from 0% (fully hydrated; i.e., mirabilite and hydrohalite) to 100% (fully anhydrous; i.e., thenardite and halite). Pure phase spectra were taken from Hanley et al. (2014), Shirley et al. (2010), and the U.S. Geological Survey spectral library (supporting information methods).

4. Results

4.1. Aqueous Geochemistry and Salt Mineralogy

Brine compositions and salt mineralogy at the springs are consistent with published data (Battler et al., 2013; Lay et al., 2013; Omelon et al., 2006; Ward & Pollard, 2018). Across all springs, fluids are dominated by sodium and chloride and contain significant concentrations of sulfate (Figure 2a and Table S1). LH brines contain the highest sulfate concentration of the three springs (60 mM) and the lowest temperature ($-3.6\ ^\circ\text{C}$). CP brines are relatively warm ($3.8\text{--}8.4\ ^\circ\text{C}$), neutral alkaline (pH 6.98–7.75) and contain higher dissolved Ca^{2+} levels than either LH or STZ (Figure 2b and Table S1). STZ brines are the most saline with

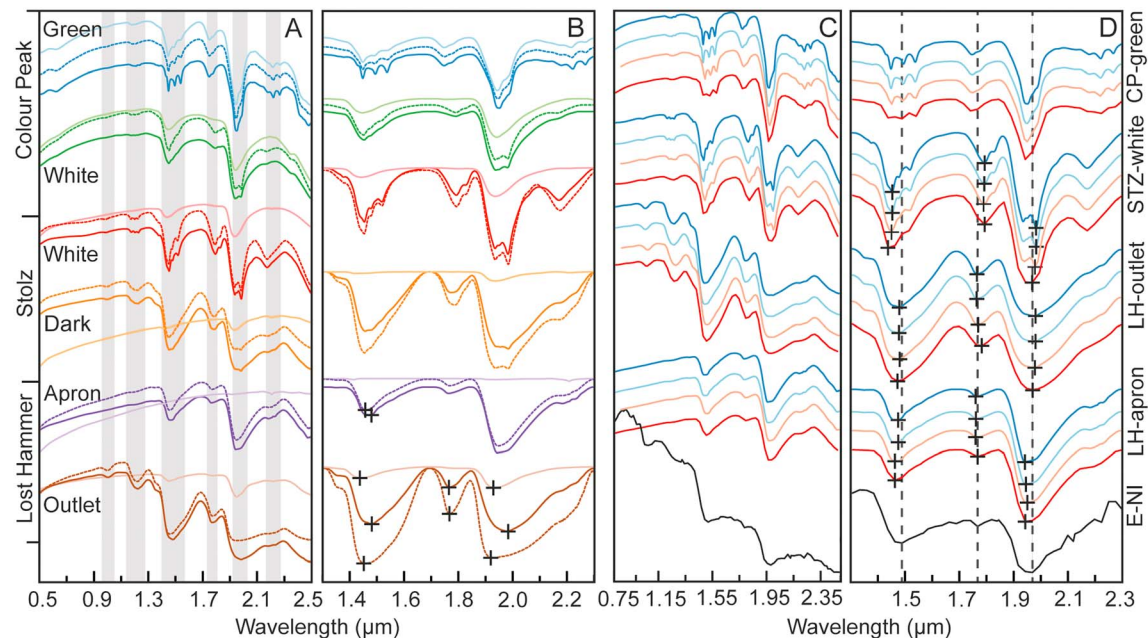


Figure 3. Representative visible near-infrared reflectance spectra of salts from the Axel Heiberg Island saline springs. Reflectance offset for clarity. (a, b) Full (a) and continuum-removed (b) spectra at 100 K (darkest), 253 K (dashed), and 293 K (lightest). Gray lines highlight H₂O/OH water bands. (c, d) Representative full (c) and continuum-removed (d) spectra resampled to instrument band passes, ordered from top to bottom: full nanometer-resolved spectra, Moons and Jupiter Imaging Spectrometer (MAJIS) resolution, Mapping Infrared Spectrometer for Europa (MISE) resolution, Near-Infrared Mapping Spectrometer (NIMS) resolution. Europa non-icy endmember spectrum (black), acquired by Galileo NIMS, is reproduced from Carlson et al. (2005). Dashed lines and crosses in (b) and (d) show the positions of absorption band minima for NIMS data and Axel Heiberg Island data, respectively. LH = Lost Hammer; STZ = Stolz; CColor Peak.

respect to sodium (3,790–3,868 mM) and chloride (5,213–5,216 mM) and possess subzero temperatures (−1.7 and −2.9 °C). Sulfide concentrations ranged from highs of 1.86 mM at CP to lows of 0.04 mM at STZ (Table S1). The δD and $\delta^{18}O$ of the spring brines plot close to the local meteoric water line (Figure 2c). LH brine shows the lowest $\delta^{18}O$ and δD values of the springs but is comparable to that of nearby permafrost. CP brine isotope values plot close to snowmelt on CP Diapir, in agreement with Pollard et al. (1999; Figure 2c). The isotopic values of two snowmelt pools sampled on STZ Diapir fall below the local meteoric water line and show higher $\delta^{18}O$ and δD than the STZ brines (Figure 2c).

Mineralogy (measured by XRD after raising samples to 20 °C) is dominated at LH by Na sulfates, notably mirabilite and thenardite, with lesser contributions from chlorides (Table S2). The low-temperature chloride hydrohalite is present in several samples, which had not previously been reported by Battler et al. (2013). White crusts at CP are dominated by halite, while dark precipitates consisted primarily of gypsum (CaSO₄·2H₂O) and calcite (CaCO₃), which are not considered likely phases at Europa. White salt assemblages at STZ contained higher abundances of Na chloride salts, predominantly anhydrous halite. The darker banded salts were composed of thenardite and halite, as approximately equal major phases.

4.2. Vis-NIR Spectral Characteristics

Representative spectra from salt precipitates at all three measured temperatures are plotted in Figure 3. The largest spectral differences are observed between 253 and 273 K. “CP green” (dark green precipitates) shows a sharpening of the major water absorption bands at 1.5 (triplet), 2.0 (doublet), and 2.2 μm (triplet) at 253 and 100 K, consistent with gypsum (Cloutis et al., 2006), which dominates this sample (Table S2) and is stable at room temperature. Spectra from “STZ white” at 253 and 100 K are consistent with hydrohalite; particularly the doublet 1.5- and 2.0-μm features (Light et al., 2016; measured at 243 K) and the 1.75-μm feature in frozen NaCl brine (Hanley et al., 2014). “STZ dark” salts display muted versions of these features. Spectra from CP white and all LH and STZ salts have minimal hydration features at 293 K, with overtone absorptions at 1.2 and 2.2 μm absent entirely. LH spectra exhibit the 2.2-μm absorption feature as a slight shoulder to the larger and broader 2.0-μm feature, consistent with the presence of mirabilite. Salts from the interior of the outlet

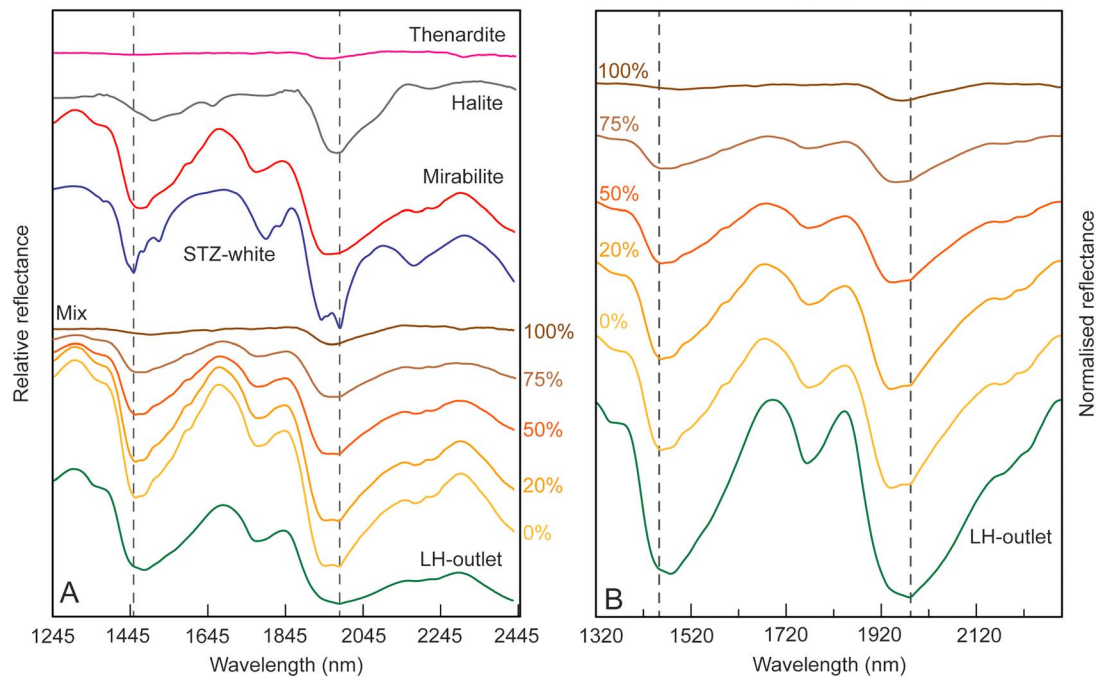


Figure 4. Comparison of numerically mixed spectra with LH outlet spectra (measured at 100 K). STZ white (at 100 K) provides the hydrohalite spectral endmember. Each mix represents an anhydrous percentage; 20% anhydrous corresponds to that measured in LH Outlet by X-ray diffraction at 20 °C. (a) Visible near-infrared reflectance spectra of spectral endmembers and their mixes. (b) Continuum-removed spectral mixes. Gray dashed lines denote the position of major hydrohalite band minima at 1,452 and 1,983 nm (visible in STZ white). STZ = Stolz; LH = Lost Hammer.

dome show broader absorptions and exhibit hydration features at 1.0 and 1.2 μm that are absent in salts from the surface of the salt apron. Numerical linear mixes failed to recreate LH spectra, even when all components identified by XRD were included (Figure 4). For example, hydrohalite details were not observed in LH spectra but were evident in spectral mixes designed to simulate LH phase abundances.

4.3. Comparisons With Mission Data

The 100-K spectra resampled to match spacecraft instrument capabilities are plotted in order of decreasing resolution in Figures 3c and 3d. Major absorption features in LH salts show similar asymmetry and broadening to the NIMS data from european non-icy material. Furthermore, minima for the 1.75- μm band in LH salts very closely match the corresponding minimum of Europa's non-icy material observed by NIMS. Band minima of the major 1.5- and 2.0- μm absorptions tend to shift to shorter wavelengths at lower spectral resolution (Figure 3d). Spectral details such as the diagnostic gypsum triplets in CP salts and the hydrohalite doublets in STZ salts (1.5 and 2.0 μm) are represented at MISE and MAJIS resolutions, but at NIMS resolution these become difficult to resolve or are absent entirely. The hydrohalite doublet at 2.0 μm in STZ white appears as a single feature at NIMS resolution with a band minimum that closely matches data from Europa.

5. Discussion

5.1. Environmental Controls on Spring Geochemistry

The AHI springs provide geochemical analogues for the formation of hydrated salt deposits from subsurface fluids on icy moons. Constraining their geologic and geochemical context as well as their stability is crucial for understanding which aspects can be extrapolated for planetary exploration. The brine $\delta^{18}\text{O}$ and δD values support the hypothesis that the AHI springs are recharged by meteoric water. Andersen et al. (2002) suggested that evaporite diapirs create conduits through permafrost that allow meteoric waters to infiltrate and dissolve deep evaporites, buffering the spring temperatures via a dynamic equilibrium between the sub-permafrost geotherm and the permafrost itself. The behavior of the STZ and LH systems is consistent with this idea. At both sites, $\delta^{18}\text{O}$ and δD values of the spring brines are significantly more depleted than local snowmelt and at LH are similar to permafrost values. This indicates a complex mechanism of water

recharge to the system, potentially including local permafrost melts and more distal meteoric sources that could have experienced a longer residence time in the evaporites. At CP, however, similar δD and $\delta^{18}O$ values in the brine and snow show that contemporary melt is likely feeding the springs, consistent with interpretations by Omelon et al. (2006). This challenges the notion (Pollard et al., 1999) that long residence times are required within the evaporites and permafrost to acquire a high solute load and to buffer the spring temperatures.

5.2. Implications for Spectroscopic Detection of Salts on Europa

The natural salts studied here show complex behaviors, not fully predictable from the behaviors of pure laboratory salts. Some samples, notably CP green, CP white, and STZ white, show sharpening of spectral detail at 253 and 100 K, predicted from pure salts. However, for most samples the main temperature-related spectral changes are associated with the loss of hydration at 293 K and not the narrowing or sharpening effects seen at low temperature with pure salts. For example, the mirabilite-dominated LH salts lack the sharpened details observed in pure mirabilite (Dalton et al., 2005), instead exhibiting smooth absorptions that span the 1.3- to 1.7- and 1.8- to 2.3- μm ranges. Achieving this “smoothing” effect in previous linear mixing efforts was achieved by adding up to 65% sulfuric acid hydrate (Carlson et al., 2005; Dalton et al., 2012). Based on LH salt spectra, which contain only Na sulfates and chloride salts (plus trace detrital quartz), “smooth” low-temperature spectra do not require the addition of sulfuric acid hydrate. This does not rule out its presence at Europa but demonstrates that it need not be such a significant component to produce the observed spectral features.

Overall, LH salt spectra measured at 100 K most closely recreate the shape, breadth, and depth of absorption features in NIMS non-icy spectra, including the 1.75- μm band minimum (Figure 3d). These data therefore are consistent with an LH-like sulfate-rich composition at Europa. However, they do not rule out the presence of chlorides salts, as data from Europa show some similarity to the chloride-rich STZ samples when viewed at the lower spectral resolution of mission data. The hydrohalite doublet at 2.0 μm in STZ white disappears at NIMS resolution, meaning that this feature would not have been detectable, even if hydrohalite were present. Recent ground-based observations with greatly improved spectral resolution (e.g., Fischer et al., 2015) lack data in the 1.80- to 1.95- μm region so also cannot be used to definitively eliminate hydrohalite. Future spacecraft instruments such as MISE (Europa Clipper) and MAJIS (JUICE) have sufficient resolution to capture this and other diagnostic features; therefore, these missions will reveal if europian non-icy deposits bear closer resemblance to a “LH-” or “STZ-like” composition.

Hydrohalite was detected in some LH samples by XRD (Table S2) as a minor phase, including LH outlet. Spectral linear mixing predicts that hydrohalite should be observable in the near infrared in this sample; however, apart from a subtle reflectance minimum at 1.983 μm , hydrohalite features were absent, even when the sample was measured at 100 K (Figure 4). Incorporating spectrally featureless anhydrous phases at proportions above 50% into the mix produces similar smoothing effects but causes features at 1.5 and 2.0 μm to lack the depth and breadth observed in LH outlet spectra (Figure 4b). Moreover, the approximate anhydrous proportion measured by XRD at room temperature (20%) provides an upper limit on anhydrous phase abundance in LH outlet material, which will be heavily hydrated at 100 K. This demonstrates that the behavior of natural assemblages, which can be complex intimate mixtures of compounds and hydrations states, cannot be predicted from the additive properties of pure salts alone. If ocean-derived hydrated chlorides are present on the surface of Europa (Hand & Carlson, 2015; Brown & Hand, 2013), they could be spectrally obscured by sulfates. Importantly, if sulfates are exogenic in origin (i.e., from Io’s plasma torus), this could present a problem for identifying endogenic material within surface deposits. In this case, the 1.983- μm band minimum could be an important diagnostic feature of hydrohalite that is retained, albeit subtly, in sulfate deposits.

5.3. Geochemical Implications for Europa From Natural Analogues

The deposits at AHI springs show that natural brines with similar major ion chemistry can precipitate different mineralogical deposits, ranging from calcite and gypsum at CP, to mirabilite and hydrohalite at LH. These differences are accounted for by minor variations in the sulfate:chloride ratio of the brines and by dissolved calcium and alkalinity (Figures 2 and S2). CP exhibits minerals not considered likely at Europa; however, their formation demonstrates how minor differences in geochemistry can produce varied mineralogies.

The same may be true on a geologically diverse world such as Europa. Additionally, CP can be a useful analogue for cryovolcanic precipitates on bodies with more alkaline and carbonate-rich aqueous chemistries, such as Enceladus (Glein et al., 2015).

The compositions of AHI deposits do not reflect equilibrium salt assemblages that would form if the spring brines fully crystallized; rather, they represent a snapshot during this evolution (Figure S2 and Table S3). For example, despite bearing a high chloride:sulfate ratio (25; Table S1), LH salts are dominated by mirabilite and thenardite, showing that a dominantly chloride brine can form sulfate-dominated deposits. Thermodynamic models show that mirabilite forms early upon freezing or evaporation-driven concentration, while chlorides are retained in late-stage brines that can be transported away from the deposit (Figure S2). On Europa, a chloride-dominated ocean in which sulfate is only a minor constituent may form sulfate-rich salt assemblages in a similar manner, at the surface or within the ice, while denser chloride-enriched brines migrate away (Zolotov & Shock, 2001). The discovery of endogenous sulfate salts on Europa would therefore not preclude a chloride-dominated ocean.

The composition of Europa's ocean is not well constrained, and the relative contributions of exogenic and endogenic processes to surface non-ice material are not known. Different geographical regions may harbor different compositions, reflecting different processes (Fischer et al., 2015). In one proposed scenario, ocean-derived chlorides are delivered to the surface and become progressively altered by exogenous sulfur ion bombardment (Brown & Hand, 2013). Under these circumstances, STZ white salts represent pristine deposits, with STZ dark and the LH salt assemblages representing more altered, sulfate-rich deposits where the vis-NIR signature of hydrohalite is obscured. Alternatively, if the ocean is sulfate rich (Kargel et al., 2000), then LH salts would represent suitable analogue material for pristine endogenic deposits. The study of natural environments such as the AHI springs forms part of an integrative theoretical, experimental, and analogue approach that will be critical to interpreting future mission data, both from upcoming flyby missions and the under-development NASA Europa Lander project.

Acknowledgments

This work was funded by the Leverhulme Trust (RPG-2016-153) and the Natural Sciences and Engineering Research Council of Canada. The Planetary Spectroscopy Facility, University of Winnipeg, is supported by the University of Winnipeg, the Canada Foundation for Innovation, the Manitoba Research Innovation Fund, and the Canadian Space Agency. Thanks to the Polar Continental Shelf Program (Natural Resources Canada) for logistical field support in Nunavut. FG was financially supported by the "HIPATIA" research program of the University of Almería. Geochemical and spectral data presented in this manuscript are available in supporting information. Finally, we thank two anonymous reviewers for constructive comments.

References

- Andersen, D. T., Pollard, W. H., McKay, C. P., & Heldmann, J. (2002). Cold springs in permafrost on Earth and Mars. *Journal of Geophysical Research*, 107(E3), 5015. <https://doi.org/10.1029/2000JE001436>
- Battler, M. M., Osinski, G. R., & Banerjee, N. R. (2013). Mineralogy of saline perennial cold springs on Axel Heiberg Island, Nunavut, Canada and implications for spring deposits on Mars. *Icarus*, 224(2), 364–381. <https://doi.org/10.1016/j.icarus.2012.08.031>
- Blaney, D. L., Clark, R., Dalton, J. B., Davies, A. G., Green, R., Hedman, M., et al. (2015). Mapping imaging spectrometer for Europa (MISE). Paper presented at European Planetary Science Congress, Nantes, France
- Bramble, M. S., Flemming, R. L., Hutter, J. L., Battler, M. M., Osinski, G. R., & Banerjee, N. R. (2014). A temperature-controlled sample stage for in situ micro-X-ray diffraction: Application to Mars analog mirabilite-bearing perennial cold spring precipitate mineralogy. *American Mineralogist*, 99(5-6), 943–947. <https://doi.org/10.2138/am.2014.4629>
- Brown, M. E., & Hand, K. P. (2013). Salts and radiation products on the surface of Europa. *The Astronomical Journal*, 145(4), 110–117. <https://doi.org/10.1088/0004-6256/145/4/110>
- Carlson, R. W., Anderson, M. S., Mehlman, R., & Johnson, R. E. (2005). Distribution of hydrate on Europa: Further evidence for sulfuric acid hydrate. *Icarus*, 177(2), 461–471. <https://doi.org/10.1016/j.icarus.2005.03.026>
- Carlson, R. W., Calvin, W. M., Dalton, J. B., Hansen, G. B., Hudson, R. L., Johnson, R. E., et al. (2009). Europa's surface composition. In R. T. Pappalardo, W. B. McKinnon, & K. Khurana (Eds.), *Europa* (pp. 283–327). Tuscon, AZ: University of Arizona Press.
- Carr, M. H., Belton, M. J., Chapman, C. R., Davies, M. E., Geissler, P., Greenberg, R., et al. (1998). Evidence for a subsurface ocean on Europa. *Nature*, 391(6665), 363–365. <https://doi.org/10.1038/34857>
- Cline, J. T. (1969). Spectrophotometric determination of hydrogen sulfide in natural waters. *Limnology and Oceanography*, 14(3), 454–458
- Cloutis, E. A., Hawthorne, F. C., Mertzman, S. A., Krenn, K., Craig, M. A., Marcino, D., et al. (2006). Detection and discrimination of sulfate minerals using reflectance spectroscopy. *Icarus*, 184(1), 121–157. <https://doi.org/10.1016/j.icarus.2006.04.003>
- Dalton, J. B. (2007). Linear mixture modeling of Europa's non-ice material based on cryogenic laboratory spectroscopy. *Geophysical Research Letters*, 34, L21205. <https://doi.org/10.1029/2007GL031497>
- Dalton, J. B., Prieto-Ballesteros, O., Kargel, J. S., Jamieson, C. S., Jolivet, J., & Quinn, R. (2005). Spectral comparison of heavily hydrated salts with disrupted terrains on Europa. *Icarus*, 177(2), 472–490. <https://doi.org/10.1016/j.icarus.2005.02.023>
- Dalton, J. B., Shirley, J. H., & Kamp, L. W. (2012). Europa's icy bright plains and dark lineae: Exogenic and endogenic contributions to composition and surface properties. *Journal of Geophysical Research*, 117, E03003. <https://doi.org/10.1029/2011JE003909>
- Fischer, P. D., Brown, M. E., & Hand, K. P. (2015). Spatially resolved spectroscopy of Europa: The distinct spectrum of large-scale chaos. *The Astronomical Journal*, 150(5), 164. <https://doi.org/10.1088/0004-6256/150/5/164>
- Fischer, P. D., Brown, M. E., Trumbo, S. K., & Hand, K. P. (2016). Spatially resolved spectroscopy of Europa's large-scale compositional units at 3–4 μm with Keck NIRSPEC. *The Astronomical Journal*, 153, 13. <https://doi.org/10.3847/1538-3881/153/1/13>
- Glein, C. R., Baross, J. A., & Waite, J. H. (2015). The pH of Enceladus' ocean. *Geochimica et Cosmochimica Acta*, 162, 202–219. <https://doi.org/10.1016/j.gca.2015.04.017>
- Hand, K. P., & Carlson, R. W. (2015). Europa's surface color suggests an ocean rich with sodium chloride. *Geophysical Research Letters*, 42, 3174–3178. <https://doi.org/10.1002/2015GL063559>

- Hanley, J., Dalton, J. B., Chevrier, V. F., Jamieson, C. S., & Barrows, R. S. (2014). Reflectance spectra of hydrated chlorine salts: The effect of temperature with implications for Europa. *Journal of Geophysical Research: Planets*, *119*, 2370–2377. <https://doi.org/10.1002/2013JE004565>
- Harrison, J. C., & Jackson, M. P. A. (2014). Exposed evaporite diapirs and minibasins above a canopy in central Sverdrup Basin, Axel Heiberg Island, Arctic Canada. *Basin Research*, *26*(4), 567–596. <https://doi.org/10.1111/bre.12037>
- Howell, S. M., & Pappalardo, R. T. (2018). Band formation and ocean-surface interaction on Europa and Ganymede. *Geophysical Research Letters*, *45*, 4701–4709. <https://doi.org/10.1029/2018GL077594>
- Jia, X., Kivelson, M. G., Khurana, K. K., & Kurth, W. S. (2018). Evidence of a plume on Europa from Galileo magnetic and plasma wave signatures. *Nature Astronomy*, *2*(6), 459–464. <https://doi.org/10.1038/s41550-018-0450-z>
- Kargel, J. S., Kaye, J. Z., Head, J. W. III, Marion, G. M., Sassen, R., Crowley, J. K., et al. (2000). Europa's crust and ocean: Origin, composition, and the prospects for life. *Icarus*, *148*(1), 226–265. <https://doi.org/10.1006/icar.2000.6471>
- Langevin, Y., Piccioni, G., & the MAJIS Team. (2013). MAJIS (Moons and Jupiter Imaging Spectrometer) for JUICE: Objectives for the Galilean satellites. Paper presented at European Planetary Science Conference, London, United Kingdom
- Lay, C.-Y., Mykytczuk, N. C. S., Yergeau, É., Lamarche-Gagnon, G., Greer, C. W., & Whyte, L. G. (2013). Defining the functional potential and active community members of a sediment microbial community in a high-Arctic hypersaline subzero spring. *Applied and Environmental Microbiology*, *79*(12), 3637–3648. <https://doi.org/10.1128/AEM.00153-13>
- Light, B., Carns, R. C., & Warren, S. G. (2016). The spectral albedo of sea ice and salt crusts on the tropical ocean of Snowball Earth: 1. Laboratory measurements. *Journal of Geophysical Research: Oceans*, *121*, 4966–4979. <https://doi.org/10.1002/2016JC011803>
- Ligier, N., Poulet, F., Carter, J., Brunetto, R., & Gourgéot, F. (2016). VLT/SINFONI observations of Europa: New insights into the surface composition. *The Astronomical Journal*, *151*(6). <https://doi.org/10.3847/0004-6256/151/6/163>
- McCord, T. B., Hansen, G. B., Matson, D. L., Johnson, T. V., Crowley, J. K., Fanale, F. P., et al. (1999). Hydrated salt minerals on Europa's Surface from the Galileo near-infrared mapping spectrometer (NIMS) investigation. *Journal of Geophysical Research*, *104*(E5), 11,827–11,851. <https://doi.org/10.1029/1999JE900005>
- Nimmo, F., & Pappalardo, R. T. (2016). Ocean worlds in the outer solar system. *Journal of Geophysical Research: Planets*, *121*, 1378–1399. <https://doi.org/10.1002/2016JE005081>
- Omelon, C. R., Pollard, W. H., & Andersen, D. T. (2006). A geochemical evaluation of perennial spring activity and associated mineral precipitates at Expedition Fjord, Axel Heiberg Island, Canadian High Arctic. *Applied Geochemistry*, *21*(1), 1–15. <https://doi.org/10.1016/j.apgeochem.2005.08.004>
- Orlando, T. M., McCord, T. B., & Grievés, G. A. (2005). The chemical nature of Europa surface material and the relation to a subsurface ocean. *Icarus*, *177*(2), 528–533. <https://doi.org/10.1016/j.icarus.2005.05.009>
- Pollard, W., Omelon, C., Anderson, D., & McKay, C. (1999). Perennial spring occurrence in the Expedition Fiord area of western Axel Heiberg Island, Canadian High Arctic. *Canadian Journal of Earth Sciences*, *36*(1), 105–120. <https://doi.org/10.1139/e98-097>
- Prockter, L. M., Shirley, J. H., Dalton, J. B., & Kamp, L. (2017). Surface composition of pull-apart bands in Argadnel Regio, Europa: Evidence of localized cryovolcanic resurfacing during basin formation. *Icarus*, *285*, 27–42. <https://doi.org/10.1016/j.icarus.2016.11.024>
- Roth, L., Saur, J., Retherford, K. D., Strobel, D. F., Feldman, P. D., McGrath, M. A., & Nimmo, F. (2014). Transient water vapor at Europa's South Pole. *Science*, *343*(6167), 171–174. <https://doi.org/10.1126/science.1247051>
- Schmidt, B. E., Blankenship, D. D., Patterson, G. W., & Schenk, P. M. (2011). Active formation of 'chaos terrain' over shallow subsurface water on Europa. *Nature*, *479*(7374), 502–505. <https://doi.org/10.1038/nature10608>
- Shirley, J. H., Dalton, J. B. III, Prockter, L. M., & Kamp, L. W. (2010). Europa's ridged plains and smooth low albedo plains: Distinctive compositions and compositional gradients at the leading side-trailing side boundary. *Icarus*, *210*(1), 358–384. <https://doi.org/10.1016/j.icarus.2010.06.018>
- Ward, M. K., & Pollard, W. H. (2018). A hydrohalite spring deposit in the Canadian high Arctic: A potential Mars analogue. *Earth and Planetary Science Letters*, *504*, 126–138. <https://doi.org/10.1016/j.epsl.2018.10.001>
- Zolotov, M. Y., & Shock, E. L. (2001). Composition and stability of salts on the surface of Europa and their oceanic origin. *Journal of Geophysical Research*, *106*(E12), 32,815–32,827. <https://doi.org/10.1029/2000JE001413>

References From the Supporting Information

- Marion, G. M., Mironenko, M. V., & Roberts, M. W. (2010). FREZCHEM: A geochemical model for cold aqueous solutions. *Computers & Geoscience*, *36*(1), 10–15. <https://doi.org/10.1016/j.cageo.2009.06.004>